Wetting and drying transitions in mean-field theory: describing the surface parameters for the theory of Nakanishi and Fisher in terms of a microscopic model

Kuipers, J.; Blokhuis, E.M.

Wetting and drying transitions in mean-field theory: Describing the surface parameters for the theory of Nakanishi and Fisher in terms of a microscopic model

Joris Kuipers, and Edgar M. Blokhuis

Citation: The Journal of Chemical Physics **131**, 044702 (2009); doi: 10.1063/1.3184613
View online: https://doi.org/10.1063/1.3184613
View Table of Contents: http://aip.scitation.org/toc/jcp/131/4
Published by the American Institute of Physics

Wetting and drying transitions in mean-field theory: Describing the surface parameters for the theory of Nakanishi and Fisher in terms of a microscopic model

Joris Kuipers[a] and Edgar M. Blokhuis
Colloid and Interface Science, Leiden Institute of Chemistry, Gorlaeus Laboratories, P.O. Box 9502, 2300 RA Leiden, The Netherlands

(Received 14 January 2009; accepted 30 June 2009; published online 22 July 2009)

The theory of Nakanishi and Fisher [Phys. Rev. Lett. **49**, 1565 (1982)] describes the wetting behavior of a liquid and vapor phase in contact with a substrate in terms of the surface chemical potential h_1 and the surface enhancement parameter g. Using density functional theory, we derive molecular expressions for h_1 and g and compare with earlier expressions derived from Landau lattice mean-field theory. The molecular expressions are applied to compare with results from density functional theory for a square-gradient fluid in a square-well fluid-substrate potential and with molecular dynamics simulations. © *2009 American Institute of Physics*.
[DOI: 10.1063/1.3184613]

I. INTRODUCTION

When two bulk liquid phases or a liquid in coexistence with its vapor are brought into contact with a substrate (solid wall) two situations can arise: either one of the two phases completely wets the substrate, that is one layer of liquid will cover the entire substrate (complete wet state), or one of the two phases will partially wet the substrate and form droplets on it (partial wet state). Changing a thermodynamic variable such as temperature may induce a transition between the two situations. This wetting transition was independently investigated by Cahn[1] and by Ebner and Saam.[2] Since then there has been a lot of experimental and theoretical work done on the nature and aspects of wetting transitions.[3–13] Among all these theories, the Nakanishi–Fisher model[6] has played a pivotal role in shaping our understanding of the wetting phase diagram.

In the Nakanishi–Fisher model, the free energy Ω describes the free energy of a fluid (liquid and or vapor) phase in contact with a solid wall. The solid wall is assumed to be present as a so-called spectator phase (the solid is unaffected by the fluid's thermodynamic state) and leads to the exclusion of the fluid in the region $z<0$, where z is the direction perpendicular to the wall. The free energy is a functional of the fluid's density $\rho(z)$:

$$\frac{\Omega[\rho]}{A} = \int_0^\infty dz\{m[\rho'(z)]^2 + \omega(\rho)\} - h_1\rho(0) + \frac{g}{2}\rho(0)^2, \quad (1)$$

where $A=\int dxdy$ is the surface area. The first term approximates the fluid's free energy by a simple square-gradient expression with coefficient m and bulk free energy density $\omega(\rho)$. For explicit calculations, we consider for $\omega(\rho)$ the Carnahan–Starling form:[14]

$$\omega(\rho) = \omega_{\mathrm{hs}}(\rho) - a\rho^2 = k_BT\rho\,\ln(\rho) + k_BT\rho\frac{(4\eta - 3\eta^2)}{(1-\eta)^2} - \mu\rho - a\rho^2, \quad (2)$$

where $\eta \equiv (\pi/6)\rho d^3$ with d being the molecular diameter, a is the usual van der Waals parameter to account for the attractive interactions between molecules, μ is the chemical potential, T is the absolute temperature, and k_B is Boltzmann's constant.

The last two terms in Eq. (1) account for the interaction of the fluid with the wall in terms of two phenomenological parameters, h_1 and g, which are termed the *surface chemical potential* and *surface enhancement parameter*, respectively. In terms of these two parameters, Fisher and Nakanishi located the crossover between first and second order transitions and reported prewetting transitions for a fluid off coexistence.[6] The assumption implicitly made is that the fluid-wall interaction is short ranged so that these terms only depend on the fluid's density in the direct vicinity of the wall, $\rho(0)\equiv\rho(z=0^+)$. For a fluid interacting with the substrate through long-ranged London dispersion forces, $V_{\mathrm{wall}}(z)\propto 1/z^3$, this assumption may very well be questioned.

To determine the surface tension, one minimizes the free energy in Eq. (1) leading to the following Euler–Lagrange equation for $\rho(z)$:[15]

$$2m\rho''(z) = \omega'(\rho), \quad (3)$$

with the boundary condition:

$$2m\rho'(0) = -h_1 + g\rho(0). \quad (4)$$

The surface tension is then calculated by inserting $\rho(z)$ into the free energy and subtracting the pressure contribution from the bulk at $z\to\infty$, $p=-\omega(\rho_b)$, where ρ_b is the bulk fluid density:

[a]Electronic mail: j.kuipers@chem.leidenuniv.nl.

$$\sigma = \int_0^\infty dz\{m[\rho'(z)]^2 + \omega(\rho) + p\} - h_1\rho(0) + \frac{g}{2}\rho(0)^2. \quad (5)$$

Our goal in this article is to understand the molecular origin of the two parameters h_1 and g in terms of the full shape of the interaction potential of the interaction between the fluid and the wall. For instance, setting the model parameters to zero in the Nakanishi–Fisher model ($h_1=0$ and $g=0$) results in constant density profiles at the value of the bulk density which is not expected if a fluid is brought in contact with a hard wall. To appreciate this point, we first investigate in Secs. II and III two routes to derive the Nakanishi–Fisher free energy expression: the Landau mean-field lattice model and density functional theory, providing us with a molecular interpretation of the model parameters h_1 and g. In Sec. IV the molecular expressions for h_1 and g are used to compare with results from a simple square-gradient model of a fluid interacting with the substrate through an attractive square-well potential. We end with a discussion of results.

II. LANDAU MEAN-FIELD LATTICE MODEL

The majority of studies regarding interfacial behavior have their roots in Landau mean-field theory. It is typically derived from a continuum limit of spin models with short-ranged molecular interactions and thus provides an interpretation of the microscopic parameters entering the theory.[16] In this section, to set the stage for the derivation using density functional theory in Sec. III, we briefly discuss the usual derivation of the microscopic expressions for h_1 and g in terms of the lattice interaction parameters.[6–8,17]

In Landau theory one assumes a semi-infinite set of discrete lattice sites, arranged in equally spaced layers labeled by an index $n=1,2,3,\ldots$. Each lattice site is occupied by a single molecule or remains vacant. The free energy for a molecule in the bulk is given by

$$\frac{d^3\Omega(\Phi)}{k_BTV} \equiv \omega(\Phi) = \Phi\ln(\Phi) + (1-\Phi)\ln(1-\Phi) - \tilde{\mu}\Phi - \chi\Phi^2, \quad (6)$$

where χ is the interaction parameter between neighboring molecules and where $\Phi \equiv Nd^3/V$ is the volume fraction of molecules, with d the lattice spacing (set equal to the molecular diameter), N the number of molecules, and V the system's volume.

For a fluid interacting with a solid wall, the volume fraction depends on the layer index, $\Phi=\Phi_n$, with the interaction between neighboring molecules given by

$$U_{\text{int}} \propto -\chi\Phi_n[\lambda\Phi_{n-1} + (1-2\lambda)\Phi_n + \lambda\Phi_{n+1}], \quad (7)$$

where $1/\lambda$ is the total number of nearest neighbors; for a cubic lattice $1/\lambda=6$. This expression is valid only when $n \geq 2$. In the first layer ($n=1$) the number of neighbors is reduced by the wall since the wall excludes all molecules for $n \leq 0$. Furthermore, one often allows for the interaction between two molecules that both lie in the first layer to be enhanced by a factor $(1+D)$. For $n=1$, one thus has

$$U_{\text{int}} \propto -\chi\Phi_1[(1-2\lambda)(1+D)\Phi_1 + \lambda\Phi_2]. \quad (8)$$

The total free energy for the lattice system is then

$$\frac{d^2\Omega[\Phi_n]}{Ak_BT} = \sum_{n=2}^{\infty}\{\omega(\Phi_n) - \lambda\chi\Phi_n[\Phi_{n-1} - 2\Phi_n + \Phi_{n+1}]\} + \omega(\Phi_1) - \lambda\chi\Phi_1\left\{\left[-2 + \frac{(1-2\lambda)}{\lambda}D\right]\Phi_1 + \Phi_2\right\} - \chi_s\Phi_1, \quad (9)$$

where the final term is added to account for the interaction of the molecules in the first layer with the wall with strength χ_s.

The Euler–Lagrange equation that minimizes Eq. (9) reads

$$\omega'(\Phi_n) = \begin{cases} 2\lambda\chi[\Phi_{n-1} - 2\Phi_n + \Phi_{n+1}], & \text{when } n \geq 2, \\ 2\lambda\chi\left\{\left[-2 + \frac{(1-2\lambda)}{\lambda}D\right]\Phi_1 + \Phi_2\right\} + \chi_s, & \\ \text{when } n = 1. & \end{cases} \quad (10)$$

Now, it is convenient to introduce an *apparent* value for Φ_0 so that one can extend the Euler–Lagrange equation in Eq. (10) to include the case $n=1$.[7,17] It directly follows that one should define Φ_0 as

$$\Phi_0 \equiv \frac{(1-2\lambda)}{\lambda}D\Phi_1 + \frac{\chi_s}{2\lambda\chi}. \quad (11)$$

The surface tension σ is derived by inserting into Ω the profile Φ_n that follows from the Euler–Lagrange equation and subtracting of the bulk contribution. One then has, using Eq. (11):

$$\tilde{\sigma} \equiv \frac{d^2\sigma}{k_BT} = \sum_{n=1}^{\infty}[\omega(\Phi_n) + \tilde{p} - \lambda\chi\Phi_n(\Phi_{n-1} - 2\Phi_n + \Phi_{n+1})] - \frac{\chi_s}{2}\Phi_1, \quad (12)$$

where $\tilde{p}$ is the (reduced) bulk pressure. This can also be written as

$$\tilde{\sigma} = \sum_{n=1}^{\infty}[\lambda\chi(\Phi_{n+1} - \Phi_n)^2 + \omega(\Phi_n) + \tilde{p}] - \chi_s\Phi_1 + \lambda\chi\left[1 - \frac{(1-2\lambda)}{\lambda}D\right]\Phi_1^2. \quad (13)$$

Next, we approximate the lattice model by taking the continuum limit. This means that we replace $\Phi_n \to \Phi(x)$, where $x \equiv z/d = x_0 + n$. In the continuum limit, we then have that

$$\Phi_{n+1} - \Phi_n \approx \Phi'(x), \quad \Phi_{n-1} - 2\Phi_n + \Phi_{n+1} \approx \Phi''(x). \quad (14)$$

Furthermore, we shall define $\Phi_1 \to \Phi(0)$, which implies that $x=n-1$, but one might consider a more judiciously chosen location of the solid wall. However, since it is not our goal to accurately approximate the lattice model, we shall not pursue this line.

In the continuum limit, the Euler–Lagrange equation in Eq. (10) becomes

$$\omega'(\Phi) = 2\lambda\chi\Phi''(x). \tag{15}$$

With $\Phi_0=\Phi_1-(\Phi_1-\Phi_0)\approx\Phi(0)-\Phi'(0)$, the boundary condition in Eq. (11) is given by

$$\Phi'(0) = \left[1 - \frac{(1-2\lambda)}{\lambda}D\right]\Phi(0) - \frac{\chi_s}{2\lambda\chi}. \tag{16}$$

Finally, the expression for the surface tension in Eq. (13) becomes

$$\tilde{\sigma} = \int_0^\infty dx\{\lambda\chi[\Phi'(x)]^2 + \omega(\Phi) + \tilde{p}\} - \chi_s\Phi(0) + \lambda\chi\left[1 - \frac{(1-2\lambda)}{\lambda}D\right]\Phi(0)^2. \tag{17}$$

This expression for the surface tension is identical to the Nakanishi–Fisher expression in Eq. (5) when the following identifications are made:

$$\frac{m}{d^5 k_B T} = \lambda\chi,$$

$$\frac{h_1}{d k_B T} = \chi_s, \tag{18}$$

$$\frac{g}{d^4 k_B T} = -2(1-2\lambda)\chi D + 2\lambda\chi.$$

One finds that h_1 is directly related to χ_s which is to be expected. The identification for g is somewhat more subtle. It is the sum of *two* terms, one term due to the enhanced interaction between molecules near the wall as described by D, and one term that is present even in the absence of any enhancement.

III. DENSITY FUNCTIONAL THEORY

In this section, we consider density functional theory with the full, nonlocal integral term to describe the pair interactions between molecules and show how it can be cast into the form of the Nakanishi–Fisher expression. The starting expression for the free energy functional reads[18]

$$\Omega[\rho] = \int d\vec{r}[\omega_{\rm hs}(\rho) + \rho(\vec{r})V_{\rm ext}(\vec{r})] + \frac{1}{2}\int d\vec{r}_1\int d\vec{r}_2 U(r)\rho(\vec{r}_1)\rho(\vec{r}_2), \tag{19}$$

where $\omega_{\rm hs}(\rho)$ is given by the expression in Eq. (2) and $U(r)$ is the *attractive part* of the interaction potential between molecules at a distance $r\equiv|\vec{r}_2-\vec{r}_1|$. The external potential $V_{\rm ext}(\vec{r})=V_{\rm ext}(z)$ models the interaction of the fluid with the solid wall. We shall assume that it is infinitely hard when $z<0$, and given by some short-ranged (usually attractive) interaction $V_{\rm ext}(z)=V_{\rm wall}(z)$ for $z>0$. As a result of the infinite repulsion, we have that $\rho(z)=0$ when $z<0$, and we can limit the integrations in Eq. (19) to the region $z>0$:

$$\frac{\Omega[\rho]}{A} = \int_0^\infty dz[\omega_{\rm hs}(\rho) + \rho(z)V_{\rm wall}(z)] + \frac{1}{2}\int_0^\infty dz_1\int_{z_2>0} d\vec{r}_2 U(r)\rho(z_1)\rho(z_2). \tag{20}$$

Next, we consider the gradient expansion for $\rho(z_2)$:

$$\rho(z_2) = \rho(z_1) + z_{12}\rho'(z_1) + \frac{z_{12}^2}{2}\rho''(z_1) + \cdots. \tag{21}$$

The gradient expansion does not take into account that $\rho(z_2)=0$ when $z_2<0$. To accommodate for this, it turns out to be convenient to extend the integration over z_2 in Eq. (20) and subtract the difference:

$$\frac{\Omega[\rho]}{A} = \int_0^\infty dz[\omega_{\rm hs}(\rho) + \rho(z)V_{\rm wall}(z)] + \frac{1}{2}\int_0^\infty dz_1\int d\vec{r}_{12}U(r)\rho(z_1)[\rho(z_1)+\cdots] - \frac{1}{2}\int_0^\infty dz_1\int_{z_2<0} d\vec{r}_2 U(r)\rho(z_1)[\rho(z_1)+\cdots]. \tag{22}$$

The final term in this expression, as well as the term containing $V_{\rm wall}(z)$, only contributes *near the wall*. In the spirit of the Nakanishi–Fisher model, we may therefore approximate $\rho(z)\approx\rho(0)$ in both these terms. With this approximation, together with the gradient expansion, one thus has

$$\frac{\Omega[\rho]}{A} = \int_0^\infty dz\{m[\rho'(z)]^2 + \omega_{\rm hs}(\rho) - a\rho(z)^2\} + \rho(0)\int_0^\infty dz V_{\rm wall}(z) - \frac{\rho(0)^2}{2}\int_0^\infty dz_1\int_{z_2<0} d\vec{r}_2 U(r), \tag{23}$$

where we have defined

$$a \equiv -\frac{1}{2}\int d\vec{r}_{12}U(r) \quad \text{and} \quad m \equiv -\frac{1}{12}\int d\vec{r}_{12}r^2U(r). \tag{24}$$

The integration over $\vec{r}_{12}$ is restricted to the region $r>d$. This is not explicitly indicated; instead, we adhere to the convention that $U(r)=0$ when $r<d$.

Comparing Eq. (23) to the Nakanishi–Fisher free energy in Eq. (1), we are finally left with the following expressions for the surface interaction parameters h_1 and g:

$$h_1 = -\int_0^\infty dz V_{\rm wall}(z),$$

$$g = -\int_0^\infty dz_1\int_{z_2<0} d\vec{r}_2 U(r) = -\frac{1}{4}\int d\vec{r}_{12}rU(r). \tag{25}$$

The structure of these expressions is similar to the results from the Landau model. The parameter h_1 is directly related to (the integral of) the wall-fluid interaction potential. For attractive interactions, h_1 is positive and wetting transitions

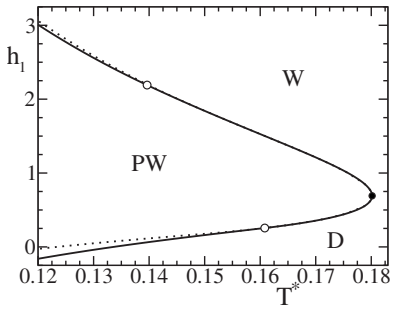

FIG. 1. Wetting phase diagram for the Nakanishi–Fisher model in terms of the surface chemical potential h_1 (in units of k_BTd) as a function of the reduced temperature $T^*=k_BTd^3/a$ ($m=ad^2/6$, $g=ad/2$). The symbols W, PW, and D mark the wetting, partial wetting, and drying region, respectively. The upper solid line is the locus of wetting transitions whereas the lower solid line is the locus of drying transitions. Open circles on these solid lines mark the locations of the tricritical points where the wetting/drying transition changes from first to second order in the direction of the liquid-vapor critical point (solid circle). The dashed lines are approximate results for the wetting and drying transitions based on the ρ^4-form of the free energy in Eq. (28).

are expected to occur with increasing h_1. The expression for g is given directly in terms of the interaction potential between fluid molecules. In this case, there is no enhancement factor—the interaction between molecules is not different at the surface then in the bulk region—and the only contribution to g comes from the "missing" fluid-fluid interaction next to the hard wall. Since $U(r)<0$ (it is the *attractive* part of the interaction between fluid molecules), one has that $g>0$ thus opposing wetting.

The absence of an enhancement factor is the consequence of the assumption of pairwise additivity of the interaction between molecules. In general, one might include three- or many-body effects occurring near the hard wall and consider a more general form for the interaction potential between molecules:

$$U(\vec{r}_1,\vec{r}_2) = U(r) + \Delta U(\vec{r}_1,\vec{r}_2). \tag{26}$$

The term $\Delta U(\vec{r}_1,\vec{r}_2)$, which accounts for the deviation from pairwise additivity, then leads to the existence of an additional contribution in the expression for g, which may be either positive or negative. It is this term that is represented by the enhancement factor D in the Landau mean-field lattice model.

In square-gradient theory, it is assumed that the fluid-fluid interactions as described by $U(r)$ are generally short-ranged. One may therefore assume that the attractive interaction does not extend significantly beyond the diameter d. In that case, Eqs. (24) and (25) lead to the following expressions for the parameters m and g in terms of the van der Waals parameter a:

$$m = \frac{ad^2}{6} \quad \text{and} \quad g = \frac{ad}{2}. \tag{27}$$

With these values for m and g, one may construct the wetting phase diagram as predicted by the Nakanishi–Fisher model. In Fig. 1, the solid lines are the loci of wetting ($h_{1,W}$) and drying ($h_{1,D}$) transitions as a function of temperature. The wetting and drying transitions turn from first to second order transitions at so-called *tricritical points*, indicated by the open circles, on approach to the liquid-vapor critical point (solid circle). In Table I we have listed numerical values for the locations of the critical point and the tricritical points in the wetting phase diagram for the various theories discussed here.

The advantage of the Nakanishi–Fisher model is that it is relatively simple to locate wetting and drying transitions and determine whether they are of first or second order. Especially the determination of the *nature* (order) of the transition is notoriously difficult in experiments, simulations and more sophisticated density functional theory calculations.[19–21] It is therefore useful to investigate the results of the Nakanishi–Fisher model to establish a first order approximation, while recognizing that more sophisticated density functional theory calculations should give more accurate results.

Furthermore, the Nakanishi–Fisher model has the advantage that analytical expressions for h_1 and g at the wetting and drying transitions may be obtained assuming proximity to the critical point, replacing the Carnahan–Starling form for $\omega(\rho)$ by a ρ^4-form:

$$\omega(\rho) = \frac{m}{(\Delta\rho)^2\xi^2}(\rho-\rho_v)^2(\rho-\rho_\ell)^2. \tag{28}$$

Minimizing the free energy in Eq. (1) using this form for $\omega(\rho)$ leads to the well-known tanh-profile for the liquid-vapor interface:

$$\rho(z) = \rho_c - \frac{\Delta\rho}{2}\tanh\left(\frac{z}{2\xi}\right), \tag{29}$$

where ξ is the bulk correlation length, $\rho_c=\frac{1}{2}(\rho_\ell+\rho_v)$ and $\Delta\rho=\rho_\ell-\rho_v$. Inserting this expression for the interfacial density profile into Eq. (5), one obtains for the surface tension of the liquid-vapor interface:

TABLE I. Listed are numerical values for the locations of the critical and tricritical points obtained in the various models (NF is the Nakanishi–Fisher model and SQW is the square-gradient fluid interacting with the substrate through a square-well potential). The location is given by the reduced temperature $T^*=k_BTd^3/a$ and the surface interaction parameter ε (in units of k_BT) or h_1 (in units of k_BTd).

	Critical point		Tricritical wetting		Tricritical drying	
	T^*	ε, h_1	T^*	ε, h_1	T^*	ε, h_1
NF	0.180 155	0.691 490	0.139 639	2.190 712	0.160 824	0.255 710
NF (ρ^4)	0.180 155	0.691 490	0.149 415	1.860 343	0.149 415	0.173 383
SQW	0.180 155	0.893 475	0.1478	2.4613	0.1248	0.0190

$$\sigma_{\ell v} = \frac{m(\Delta\rho)^2}{3\xi}. \tag{30}$$

The surface tensions for the solid-liquid and solid-vapor interfaces are obtained by minimizing Eq. (1) taking into account the boundary condition at the substrate, Eq. (4), and inserting the corresponding density profiles into Eq. (5). Using Young's equation, $\sigma_{sv}=\sigma_{s\ell}+\sigma_{\ell v}\cos(\theta)$, one is then able to determine whether the surface is (partially) wet or dry upon changing h_1 and g. For a *second order* wetting or drying transition, one explicitly has

$$g = \frac{2m}{\xi} = \frac{6\sigma_{\ell v}}{(\Delta\rho)^2},$$

$$h_{1,W} = g\rho_\ell = \frac{6\sigma_{\ell v}\rho_\ell}{(\Delta\rho)^2}, \tag{31}$$

$$h_{1,D} = g\rho_v = \frac{6\sigma_{\ell v}\rho_v}{(\Delta\rho)^2}.$$

The loci of the wetting and drying transitions determined using the ρ^4-form for $\omega(\rho)$ are drawn in Fig. 1 as the dashed lines. The correspondence near the critical point is good as to be expected. The corresponding tricritical points for both the wetting and drying transitions are located at a reduced temperature of $T^*=k_BTd^3/a=0.149415$, which is in between the tricritical point temperatures obtained using the full Carnahan-Starling form for $\omega(\rho)$ (see Table I).

In Sec. IV, we compare the wetting phase diagram in Fig. 1 to the wetting phase diagram obtained for a square-gradient fluid interacting with the substrate through an attractive square-well potential.

IV. SQUARE-GRADIENT FLUID IN A SQUARE-WELL POTENTIAL

In this section our goal is to show how the results of the Nakanishi–Fisher model can be used together with Eq. (25) to predict the wetting phase diagram of more complicated density functional theories. As an example, we determine the wetting phase diagram for a square-gradient fluid interacting with the substrate through an attractive square-well potential.

Within the square-gradient approximation, the free energy of a fluid in the presence of an external potential takes on the form

$$\frac{\Omega[\rho]}{A} = \int_{-\infty}^{\infty} dz\{m[\rho'(z)]^2 + \omega(\rho) + \rho(z)V_{\text{ext}}(z)\}, \tag{32}$$

where we recall that $\omega(\rho)=\omega_{\text{hs}}(\rho)-a\rho^2$ [Eq. (2)]. For the external potential, we take the following square-well form

$$V_{\text{ext}}(z) = \begin{cases} V_0 & \text{when } z<0, \\ -\varepsilon & \text{when } 0<z<d, \\ 0 & \text{when } z>d, \end{cases} \tag{33}$$

where the limit $V_0\to\infty$ is considered. One may show that in this limit one has[3,4,22]

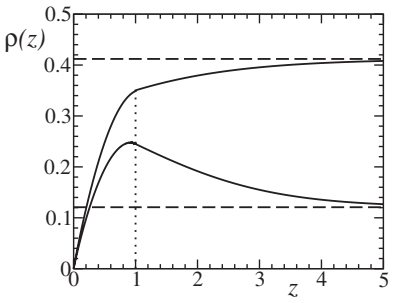

FIG. 2. Solid-liquid (upper) and solid-vapor (lower) density profiles $\rho(z)$ (in units of $1/d^3$) as a function of z (in units of d) for the square-gradient fluid interacting with the substrate via a square-well potential at a temperature $T^*=k_BTd^3/a=0.17$ and depth of the attractive well $\varepsilon/k_BT=1.2$. The horizontal dashed lines mark the values of the bulk liquid and vapor densities.

$$\rho(z=0^+) = 0. \tag{34}$$

With the observation that $\rho(z)=0$ in the whole region $z<0$, the density profile that minimizes the free energy in Eq. (32) is obtained from solving the following differential equations [with $\rho(0)=0$ as boundary condition]:

$$m\rho'(z)^2 = \begin{cases} \omega(\rho)+p-\varepsilon\rho(z)+\varepsilon\rho_d & \text{when } 0<z<d, \\ \omega(\rho)+p & \text{when } z>d, \end{cases} \tag{35}$$

where we have defined $\rho_d\equiv\rho(d)$.

Solutions for the density profile are obtained numerically using the fourth order Runge–Kutta method.[23] Two different types of solutions are found: density profiles that are monotonically increasing and density profiles that exhibit a maximum. In Fig. 2 a typical example of two such solutions is shown.

The surface tension is obtained by inserting the density profile into the expression for the free energy in Eq. (32). When the profile monotonically increases, the surface tension is given by

$$\sigma = -\varepsilon d\rho_d + 2m^{1/2}\int_0^{\rho_d} d\rho[\omega(\rho)+p-\varepsilon\rho+\varepsilon\rho_d]^{1/2} + 2m^{1/2}\int_{\rho_d}^{\rho_b} d\rho[\omega(\rho)+p]^{1/2}, \tag{36}$$

with ρ_b denoting the bulk fluid density far from the substrate which can be either ρ_ℓ to give σ_{sl} or ρ_v to give σ_{sv}. When the profile exhibits a maximum, say at $z=z_{\max}$, the surface tension is given by

$$\sigma = -\varepsilon d\rho_d + 2m^{1/2}\int_0^{\rho_{\max}} d\rho[\omega(\rho)+p-\varepsilon\rho+\varepsilon\rho_d]^{1/2} + 2m^{1/2}\int_{\rho_d}^{\rho_{\max}} d\rho[\omega(\rho)+p-\varepsilon\rho+\varepsilon\rho_d]^{1/2} + 2m^{1/2}\int_{\rho_b}^{\rho_d} d\rho[\omega(\rho)+p]^{1/2}, \tag{37}$$

with $\rho_{\max}=\rho(z=z_{\max})$.

With the surface tensions thus determined, using Young's equation for the contact angle, we are again able to

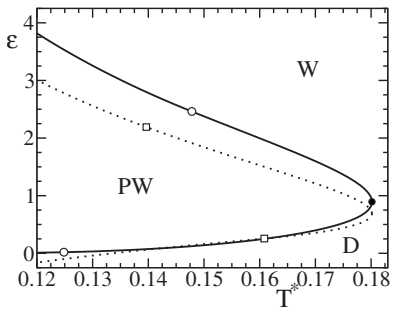

FIG. 3. Wetting phase diagram for the square-gradient fluid interacting with the substrate via a square-well potential in terms of the square-well depth ε (in units of k_BT) as a function of the reduced temperature $T^*=k_BTd^3/a$. As in Fig. 1, the symbols W, PW, and D mark the wetting, partial wetting, and drying regions, respectively; the solid lines are the loci of the wetting and drying transitions, and the open circles mark the locations of the tricritical points. The dotted lines are the Nakanishi and Fisher model results of Fig. 1, with $h_1=\varepsilon d$, with the corresponding tricritical points indicated by the open squares.

determine the wetting phase diagram which is shown in Fig. 3. The solid lines are the loci of wetting and drying transitions as a function of temperature, with the tricritical points indicated by the open circles (see Table I for numerical values).

To compare these results with the Nakanishi–Fisher model, we use the fact that the interaction is short ranged, giving $m=ad^2/6$ and $g=ad/2$ [Eq. (27)], and that $h_1=\varepsilon d$ for the square-well potential [Eq. (25)]. The wetting and drying transition lines obtained from the theory of Nakanishi and Fisher are shown in Fig. 3 as the dotted lines, with the corresponding tricritical points indicated by open squares. Reasonable agreement between the two models is obtained; the wetting transition line obtained in the square-well model is somewhat above the Nakanishi–Fisher wetting line, whereas the location of the drying transition line seems to be in better agreement. The locations of the wetting transition tricritical points are comparable but the (temperature) location of the drying tricritical points differ significantly, indicating that its location is very sensitive to the details of the model.

When the transition is of second order (close to the critical point), the location of the wetting ($\varepsilon=\varepsilon_W$) or drying transition ($\varepsilon=\varepsilon_D$) is determined by the following integral condition:

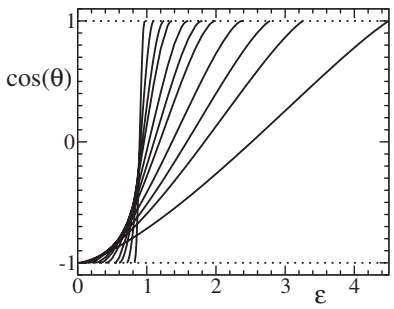

FIG. 4. Cosine of the contact angle for the square-gradient fluid interacting with the substrate via a square-well potential versus the square-well depth ε (in units of k_BT) for various wetting isotherms: $T^*=k_BTd^3/a$=0.18, 0.179, 0.177, 0.175, 0.17, 0.165, 0.16, 0.15, 0.14, 0.13, 0.11, from (top) left to right.

$$m^{1/2}\int_0^{\rho_b} d\rho[\omega(\rho)+p-\varepsilon\rho+\varepsilon\rho_b]^{-1/2}=d, \tag{38}$$

where ρ_b is either ρ_ℓ or ρ_v to determine ε_W or ε_D, respectively. This equation can be used to, numerically, determine the shape of the wetting phase very accurately. In an expansion in $t\equiv 1-T/T_c$, with T_c the critical point temperature, one obtains

$$\frac{\varepsilon_c}{k_BT}\equiv\frac{\varepsilon_W+\varepsilon_D}{2k_BT}\simeq 0.893\,475+1.7328t+\cdots,$$
$$\frac{\Delta\varepsilon}{k_BT}\equiv\frac{\varepsilon_W-\varepsilon_D}{k_BT}\simeq 4.8793t^{1/2}+\cdots. \tag{39}$$

In Fig. 4, the contact angle of the square-gradient fluid interacting with the substrate through a square-well potential is shown for a number of different isotherms.

It can be inferred from Fig. 4 that $\cos(\theta)$ jumps discontinuously from -1 to 1 at the critical point, located at $\varepsilon\simeq 0.893475$ (see Table I). Close to the critical point, i.e., when both $|\varepsilon-\varepsilon_c|\ll\varepsilon_c$ and $\Delta\varepsilon\ll\varepsilon_c$, the functional dependence of the contact angle as a function of the well depth between the limits $\varepsilon_D<\varepsilon<\varepsilon_W$ can be determined analytically, yielding

$$\cos(\theta)=3\left(\frac{\varepsilon-\varepsilon_c}{\Delta\varepsilon}\right)-4\left(\frac{\varepsilon-\varepsilon_c}{\Delta\varepsilon}\right)^3. \tag{40}$$

The same scaling form for the functional behavior of the contact angle close to the critical point is to be expected for other mean-field models. This was explicitly verified for the Nakanishi–Fisher model replacing ε by h_1 as the parameter describing the strength of the interaction of the fluid with the substrate.

A. Simulation results by van Swol and Henderson

Although it is not the goal in this article to come to a numerically accurate description of simulation results for wetting and drying, it is perhaps interesting to compare with molecular dynamics (MD) simulations carried out by van Swol and Henderson, already some 15 years ago.[11] In these simulations the wetting phase behavior and interfacial structure of a square-well fluid adsorbed at a square-well wall was investigated. The simulations are performed along a single isotherm at liquid-vapor coexistence, which the authors report to be at $T/T_c=0.738$. To compare with the liquid-vapor coexistence using the Carnahan–Starling expression for the bulk free energy, different criteria can be used to fix the location in the liquid-vapor phase diagram. Here we have chosen to fix the liquid-vapor bulk density difference $\Delta\rho$ to the value obtained in the simulations. This gives $T/T_c=0.745$ ($T^*=0.134$) and for the bulk densities $\rho_vd^3=0.027$ and $\rho_\ell d^3=0.642$, which are comparable to the densities obtained in the simulations, $\rho_vd^3=0.033$ and $\rho_\ell d^3=0.648$.

The MD simulation results by van Swol and Henderson for the contact angle as a function of the square-well depth ε are plotted in Fig. 5 as the open circles. The data clearly suggest that the wetting transition is of first order, although it is indicated by the authors that the simulations near the wet-

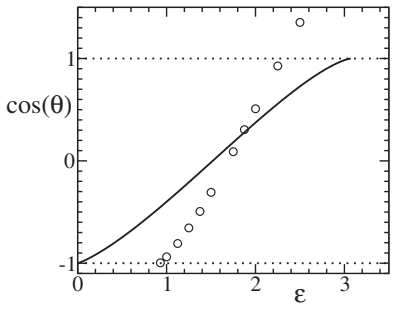

FIG. 5. Cosine of the contact angle versus the square-well depth ε (in units of k_BT) for the simulation results of Ref. 11 (open circles) and the Nakanishi–Fisher model with $h_1=\varepsilon d/2$ and $T^*=0.134$ ($m=(211/760)ad^2$, $g=(195/304)ad$).

ting transition are somewhat less reliable due to the unacceptably long simulation runs.[11] The determination of the order of the drying transition is (notoriously) difficult and it was concluded that it is either second order or very weakly first order.

To compare with the Nakanishi–Fisher model, we first use Eqs. (24) and (25) for the square-well interaction potential between fluid molecules to determine that $m=(211/760)ad^2$ and $g=(195/304)ad$. Furthermore, we use Eq. (25) for the square-well interaction potential between the fluid and the substrate to determine that $h_1=\varepsilon d/2$. The resulting behavior of the contact angle versus ε is shown as the solid in line in Fig. 5. Both the wetting and drying transition is of first order, in line with the simulation results. A striking difference between the simulation results and the Nakanishi–Fisher model is the location of the drying transition. For the Nakanishi–Fisher model, but also for the square-gradient model with the square-well fluid-substrate interaction and more sophisticated density functional theories,[11] the drying transition occurs at a value of h_1, or equivalently ε, that is close to zero at moderate temperatures not too close to the critical point. In the simulations, however, the substrate remains dry not until a large (threshold) value for the attractive surface interaction parameter (h_1 or ε) is reached.

V. DISCUSSION

As long as the interaction potential between a liquid and a substrate is short ranged—an assumption which may not be appropriate in the case of long-ranged London dispersion forces—the theory of Nakanishi and Fisher provides an excellent starting point in describing wetting behavior. We have used density functional theory to derive microscopic expressions for the surface parameters h_1 and g that are present in the Nakanishi and Fisher model. One finds that the parameter h_1 captures the interaction of the substrate with the liquid: increasing the strength of the attractive interaction (larger values of h_1) promotes wetting. The enhancement parameter g is generally determined by the sum of two contributions: (1) due to the fact that the interaction potential between fluid molecules might be enhanced near the substrate as compared to the bulk; (2) due to the lack of fluid molecules for $z<0$. Even when the fluid-fluid interaction potential is translationally invariant, as it is in the density functional theory considered here, one therefore has a nonzero, positive value for g so that the term *enhancement* parameter is somewhat misleading.

As an example, we have determined the wetting phase diagram for a square-gradient fluid interacting via a short-ranged square-well potential in terms of the square-well depth and temperature. Loci of wetting and drying transitions are obtained on which tricritical points are located where the order of the transition changes from first to second order (see Table I). Using the microscopic expressions for the surface parameters h_1 and g, the phase diagram is compared to the phase diagram from the theory of Nakanishi and Fisher. One finds that the shape of the phase diagrams are comparable (see Fig. 3) but that the location of the drying tricritical point depends sensitively on the details of the model considered.

The square-gradient model is in many ways too simplistic to describe wetting phenomena in a *quantitative* way, especially away from the critical point.[24,25] It is unfit to describe the phenomenon of surface layering[26] that is present in integral theories[27] and which also has been observed in Monte Carlo simulations.[28] Furthermore, the square-gradient model always leads to a zero density at a hard wall, which is inconsistent with the wall theorem.[22,29] However, the square-gradient model *does* have the advantage of being simple enough to be able to unambiguously determine the *order* of the wetting and drying transitions—something that may be difficult to achieve in more sophisticated density functional theories—thus allowing for a direct test of our microscopic expressions for h_1 and g by making the comparison with the theory of Nakanishi and Fisher.

[1] J. W. Cahn, J. Chem. Phys. **66**, 3667 (1977).
[2] C. Ebner and W. F. Saam, Phys. Rev. Lett. **38**, 1486 (1977).
[3] G. F. Teletzke, L. E. Scriven, and H. T. Davis, J. Colloid Interface Sci. **87**, 550 (1982).
[4] R. E. Benner, Jr., L. E. Scriven, and H. T. Davis, Faraday Symp. Chem. Soc. **16**, 169 (1981).
[5] R. Pandit and M. Wortis, Phys. Rev. B **25**, 3226 (1982).
[6] H. Nakanishi and M. E. Fisher, Phys. Rev. Lett. **49**, 1565 (1982).
[7] H. Nakanishi and M. E. Fisher, J. Chem. Phys. **78**, 3279 (1983).
[8] K. Binder, in *Phase Transitions and Critical Phenomena*, edited by C. Domb and J. L. Lebowitz (Academic, London, 1984), Vol. 8.
[9] S. Leibler and L. Peliti, Phys. Rev. B **29**, 1253 (1983).
[10] D. J. Durian and C. Franck, Phys. Rev. Lett. **59**, 555 (1987).
[11] F. van Swol and J. R. Henderson, Phys. Rev. A **40**, 2567 (1989); **43**, 2932 (1991).
[12] S. Dhawan, M. E. Reimel, L. E. Scriven, and H. T. Davis, J. Chem. Phys. **94**, 4479 (1991).
[13] S. Perković, E. M. Blokhuis, and G. Han, J. Chem. Phys. **102**, 400 (1995).
[14] N. F. Carnahan and K. E. Starling, J. Chem. Phys. **51**, 635 (1969).
[15] J. S. Rowlinson and B. Widom, *Molecular Theory of Capillarity* (Clarendon, Oxford, 1982).
[16] L. D. Landau and E. M. Lifshitz, *Statistical Physics*, 3rd ed. (Pergamon, Oxford, 1980), Vol. 5.
[17] D. E. Sullivan and M. M. Telo da Gama, in *Fluid Interfacial Phenomena*, edited by A. Croxton (Wiley, New York, 1986).
[18] R. Evans, in *Fundamentals of Inhomogeneous Fluids*, edited by D. Henderson (Dekker, New York, 1992).
[19] D. E. Sullivan, Phys. Rev. B **20**, 3991 (1979).
[20] R. Evans and P. Tarazona, J. Chem. Phys. **80**, 587 (1984).
[21] M. J. P. Nijmeijer, A. F. Bakker, C. Bruin, and J. M. J. van Leeuwen, Physica A **160**, 166 (1989).
[22] E. M. Blokhuis and J. Kuipers, J. Chem. Phys. **126**, 054702 (2007).
[23] R. L. Burden, J. D. Faires, and A. C. Reynolds, *Numerical Analysis*, 2nd ed. (Prindle, Weber & Schmidt, New York, 1981).

[24] D. M. Kroll and T. F. Meister, Phys. Rev. B **31**, 392 (1985).
[25] G. F. Teletzke, L. E. Scriven, and H. T. Davis, J. Chem. Phys. **78**, 1431 (1983).
[26] R. Evans, Mol. Phys. **42**, 1169 (1981).
[27] C. Ebner, W. F. Saam, and D. Stroud, Phys. Rev. A **14**, 2264 (1976).
[28] J. E. Lane, T. H. Spurling, B. C. Freasier, J. W. Perram, and E. R. Smith, Phys. Rev. A **20**, 2147 (1979).
[29] J. L. Lebowitz, Phys. Fluids **3**, 64 (1960).